Band-rejection filtering based on lossy torsional acousto-optic coupling in a single polarization fiber

Du-Ri Song,[1] Kwang Jo Lee,[2,*] and Byoung Yoon Kim[1]

[1]*Department of Physics, Korea Advanced Institute of Science and Technology, 373-1, Daejeon, 305-701, South Korea*

[2]*Department of Applied Physics, College of Applied Science, Kyung Hee University, Yongin-si, 446-701, South Korea*

[*]*kjlee88@khu.ac.kr*

Abstract: We propose and demonstrate novel band-rejection filtering scheme based on lossy torsional acousto-optic (AO) coupling in a single polarization fiber. Simulation results show that the polarization insensitive notch depth of −30dB is achievable for a 2-m-long fiber in the state-of-the-art fiber manufacturing technology. More efficient band-rejection in excess of −44dB could be also feasible in practical fiber length. Good agreement between our numerical simulations and proof-of-principle experiments is obtained in optical communication C-band. The measured notch depth is −29.4dB for a low loss polarization mode after propagating an AO interaction length of 49.8 cm. The filtered wavelength could be tuned linearly by the variable acoustic transducer frequency with the slope of 0.61 nm/kHz, and the polarization dependence of notch depth was measured to 0.8dB in our setup. Our experiments confirm the validity and practicality of the approach, and illustrate the in-fiber torsional AO band-rejection filter with simpler device configuration is achievable.

OCIS codes: (060.2310) Fiber optics; (230.1040) Acousto-optical devices.

References and links

1. H. S. Kim, S. H. Yun, I. K. Kwang, and B. Y. Kim, "All-fiber acousto-optic tunable notch filter with electronically controllable spectral profile," Opt. Lett. **22**(19), 1476–1478 (1997).
2. K. J. Lee, H. C. Park, and B. Y. Kim, "Highly efficient all-fiber tunable polarization filter using torsional acoustic wave," Opt. Express **15**(19), 12362–12367 (2007).
3. M. Berwick, C. N. Pannell, P. St. J. Russell, and D. A. Jackson, "Demonstration of birefringent optical fibre frequency shifter employing torsional acoustic waves," Electron. Lett. **27**(9), 713–715 (1991).
4. H. E. Engan, "Analysis of polarization-mode coupling by acoustic torsional waves in optical fibers," J. Opt. Soc. Am. A **13**(1), 112–118 (1996).
5. K. J. Lee, I.-K. Hwang, H. C. Park, and B. Y. Kim, "Polarization independent all-fiber acousto-optic tunable filter using torsional acoustic wave," IEEE Photon. Technol. Lett. **22**(8), 523–525 (2010).
6. K. J. Lee, I.-K. Hwang, H. C. Park, K. H. Nam, and B. Y. Kim, "Analyses of unintentional intensity modulation in all-fiber acousto-optic tunable filters," Opt. Express **18**(5), 3985–3992 (2010).
7. K. J. Lee, I.-K. Hwang, H. C. Park, and B. Y. Kim, "Polarization-coupling all-fiber acousto-optic tunable filter insensitive to fiber bend and physical contact," Opt. Express **17**(8), 6096–6100 (2009).
8. D. A. Satorius, T. E. Dimmick, and G. L. Burdge, "Double-pass acoustooptic tunable bandpass filter with zero frequency shift and reduced polarization sensitivity," IEEE Photon. Technol. Lett. **14**(9), 1324–1326 (2002).
9. M. S. Kang, H. S. Park, and B. Y. Kim, "Two-mode fiber acousto-optic tunable bandpass filter with zero frequency-shift," IEEE Photon. Technol. Lett. **18**(15), 1645–1647 (2006).
10. W. Zhang, L. Huang, F. Gao, F. Bo, L. Xuan, G. Zhang, and J. Xu, "Tunable add/drop channel coupler based on an acousto-optic tunable filter and a tapered fiber," Opt. Lett. **37**(7), 1241–1243 (2012).
11. W. Zhang, L. Huang, F. Gao, F. Bo, G. Zhang, and J. Xu, "Tunable broadband light coupler based on two parallel all-fiber acousto-optic tunable filters," Opt. Express **21**(14), 16621–16628 (2013).
12. B. M. Beadle and J. Jarzynski, "Measurement of speed and attenuation of longitudinal elastic waves in optical fibers," Opt. Eng. **40**(10), 2115–2119 (2001).
13. A. W. Snyder and J. Jove, *Optical Waveguide Theory* (Springer, 1983).

#220268 - $15.00 USD Received 1 Aug 2014; revised 18 Sep 2014; accepted 19 Sep 2014; published 24 Sep 2014

14. K. J. Lee, K. S. Hong, H. C. Park, and B. Y. Kim, "Polarization coupling in a highly birefringent photonic crystal fiber by torsional acoustic wave," Opt. Express **16**(7), 4631–4638 (2008).
15. D. Östling and H. E. Engan, "Narrow-band acousto-optic tunable filtering in a two-mode fiber," Opt. Lett. **20**(11), 1247–1249 (1995).

1. Introduction

In-fiber wavelength selective acousto-optic (AO) coupling has shown a great potential to realize wavelength tunable optical filters [1]. Fiber-based AO tunable filters (AOTFs) offer a number of attractive features above other typical implementations employing either thin film coatings or fiber gratings such as fiber Bragg gratings (FBGs) and long period fiber gratings (LPFGs); the prospect of wide (~100 nm) and fast (< 100 μs) wavelength tunability and variable filter transmission by simple electric control [1, 2]. Flexural and torsional acoustic waves have both been exploited for various types of all-fiber AOTFs, where they cause the resonant coupling between spatial modes in a few-mode optical fiber (for flexural wave) [1], or two eigen-polarization modes in a highly birefringent (HB) fiber (for torsional wave) [2, 3].

All-fiber torsional AOTFs have extra advantages relative to their flexural counterparts; no spectral deterioration due to acoustic birefringence [4], low polarization dependence [5], low power fluctuation [6], and immunity to external perturbation such as fiber bending or physical contact [7]. Another intriguing feature of torsional AOTFs is simple reconfiguration between notch (i.e. band-rejection) and band-pass types [2, 5]. In torsional AOTFs, the polarization mode at its resonance can be either rejected or selected by adjusting the output polarizer angle, so that the filtering type can be readily switched between notch and band-pass types in a single device configuration. In flexural AOTFs, however, it is challenging to implement both filtering types into a single configuration because additional inflexible constituents assisting AO mode coupling – such as core mode blockers inscribed in fibers [8] or a Sagnac loop with spatial mode selective couplers [9] – should be built in the filters for band-pass filtering, while notch type filtering requires only a single fiber strand for AO coupling. In general, fabrication of these additional constituents requires time-consuming and delicate post-processing of the fiber, and thus imposes a limit on practicality and mass-productivity of the devices. In respect of band-rejection filtering only, the flexural AOTFs using a single fiber strand appear to have a relative merit as compared to their torsional counterparts due to their simpler configuration [1], but it is still desirable to develop band-rejection type torsional AOTFs with simpler structures to fully exploit their superior advantages above flexural counterparts as described above.

In this paper, we report a novel approach for wavelength notch filtering based on lossy torsional AO coupling in a single polarization fiber that functions as a polarizer itself as well as AO interaction region. The proposed scheme is expected to have simpler configuration not requiring any extra polarizer or acoustic damper that are essential composition of the previous torsional AOTFs [2, 5]. Zhang *et al*. reported an add/drop operation based on evanescent coupling in flexural configurations using either a tapered fiber [10] or a pair of two individual flexural AOTFs [11]. In these cases, extra post-processing such as fiber tapering or side etching of a fiber are still required. In addition, since the evanescent coupling part is sensitive to environmental changes, the devices should be well-packaged to keep long-term stability as well as durability. In contrast, the torsional configuration adopted here has much simpler structure using only a single strand of fiber that does not require any post-processing. It should be noted that torsional AOTFs are also robust against physical perturbations relative to their flexural counterparts in general. The device presented in this paper also shows better filtering performance in its bandwidth and insertion loss, as will be described in the following sections. The merits of the approach described in this paper include long-term stability, durability, practicality, and mass-productivity. This paper is organized as follows. We will describe in detail the theoretical model developed for this particular scheme, and then experimentally validate our model. The difference in transmission properties between the proposed scheme and the previously reported torsional AOTF using a typical HB fiber will be

#220268 - $15.00 USD Received 1 Aug 2014; revised 18 Sep 2014; accepted 19 Sep 2014; published 24 Sep 2014

also discussed. Based on the additional simulation results, band-rejection efficiency at resonance and the spectral evolution of resonance dip with the fiber length will be compared.

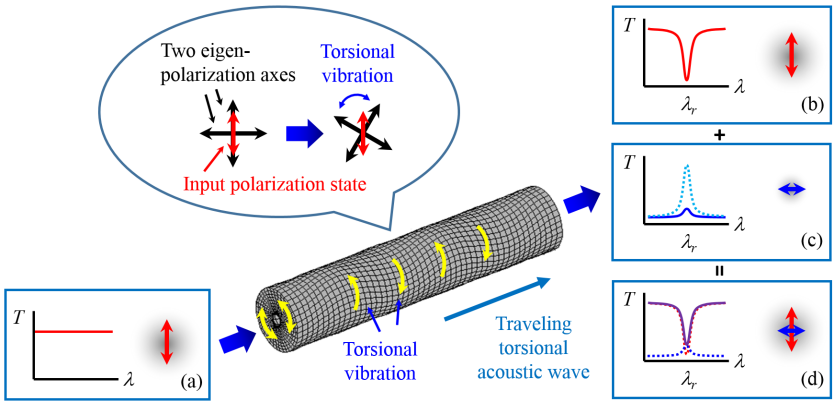

Fig. 1. Schematic diagram of the proposed band-rejection filtering scheme based on torsional AO coupling in a single polarization HB fiber. The input polarization state is set to be parallel to the polarization axis of propagation mode.

2. Theoretical model

Figure 1 shows the schematic diagram of the proposed band-rejection filtering scheme based on torsional AO coupling in a single polarization fiber, where one of the eigen-polarization mode suffers high propagation loss (lossy mode, denoted as horizontal blue arrows). The input light is linearly polarized parallel to the polarization axis of the other eigen-mode (propagation mode, denoted as red vertical arrows). Examples of input and output spectra of interacting modes are also depicted in insets of Fig. 1. The traveling torsional acoustic wave periodically twists the fiber in the circumferential direction and thus of which two eigen-polarization axes as well, so that the input propagation mode is perturbed and coupled to the other lossy eigen-mode at the resonant wavelength (λ_r) satisfying the phase matching condition:

$$\Lambda = L_B(\lambda) = \frac{\lambda}{\Delta n(\lambda)}, \tag{1}$$

where Δn, L_B, Λ, and λ denote the modal birefringence between two eigen-polarization modes, the polarization beat-length, and the acoustic and optical wavelengths, respectively. Λ is given by a variable radio frequency (RF) signal to generate the acoustic wave, which determines λ_r as indicated in Eq. (1), resulting in wavelength tunability of the filter. Figures 1(a) and 1(b) show the optical spectra of the input (vertically polarized) broadband light and the uncoupled propagation mode with the same polarization state after passing through the fiber with the minimum loss, respectively. The coupled, horizontally polarized lossy mode undergoes high propagation loss, so that its power decreases while propagating along the fiber as illustrated in Fig. 1(c). Since no output polarizer is used at the fiber end, the output filter spectrum is given by the sum of each polarization mode spectra, i.e. Figures 1(b) and 1(c), resulting in wavelength notch (or band-rejection filtering) as shown in Fig. 1(d). Here, the red and blue dotted lines correspond to each polarization mode spectra in Figs. 1(b) and 1(c), respectively. Note that the proposed scheme is working without any additional polarizer because in our scheme the fiber used for AO interaction operates as a polarizer itself as well. The coupled light diminishes due to the propagation loss, not through any extra output polarizer as was in the case of previous torsional AOTFs. In addition, when the lossy mode can be extinguished completely within a certain fiber length that is still short enough to neglect the acoustic attenuation, this scheme is also valid without an acoustic damper. In general, the damper in fiber-based AOTFs is used to define the AO interaction length well for

#220268 - $15.00 USD Received 1 Aug 2014; revised 18 Sep 2014; accepted 19 Sep 2014; published 24 Sep 2014

obtaining designed filter bandwidths and efficiencies. The acoustic power should be also damped down rapidly at which, with a minimum acoustic reflection, otherwise undesirable small signals oscillating with the harmonic frequencies of applied RF frequency can be mixed in the filtered signals [6]. In the proposed scheme, the AO interaction region is defined as the fiber length after which the lossy mode decays completely, rather than as the finite region limited by the position of the damper. So if the fiber length for efficient AO coupling is short enough to neglect the acoustic attenuation (< 10 m, typically [12]), the damper is not required to define the AO interaction region, L. The acoustic power after L is expected to be fully attenuated in either the fiber jacket or the cable sheaths, but for some particular applications where temporal stability in transmitted power is crucial, the UV epoxy bonding will be useful to minimize the harmonic oscillations of the filtered signal [6].

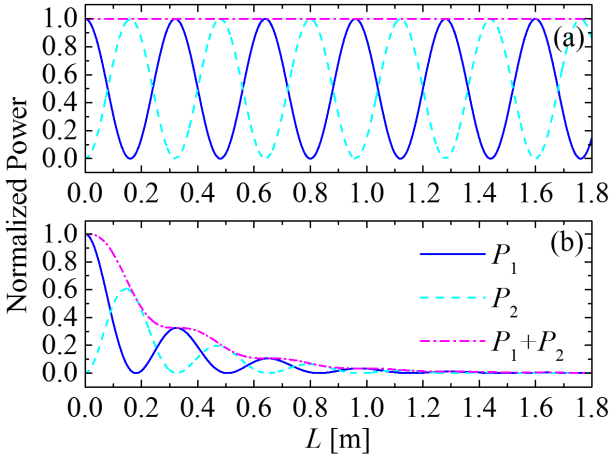

Fig. 2. Calculated modal powers plotted as a function of the propagation length L when (a) $\alpha_1 = \alpha_2 = 0$, and (b) $\alpha_1 = 0$, $\alpha_2 = 30$ dB/m. The blue solid, cyan dashed, magenta dash-dotted lines denote the modal powers of vertically polarized input mode, horizontally polarized coupled mode, and sum of each mode, respectively.

Under the slowly varying envelope approximation, the coupled-mode equations describing torsional AO coupling in a single polarization fiber can be derived as follows [13]:

$$\begin{aligned} \frac{dE_1(z)}{dz} &= -\frac{\alpha_1}{2}E_1(z) - i\kappa E_2(z)e^{i\Delta\beta z}, \\ \frac{dE_2(z)}{dz} &= -\frac{\alpha_2}{2}E_2(z) - i\kappa E_1(z)e^{-i\Delta\beta z}, \end{aligned} \tag{2}$$

where $E_1(z)$ and $E_2(z)$ are the normalized complex electric fields of the propagation and lossy eigen-polarization modes, respectively. Each α and κ also denote the linear propagation loss coefficients for the corresponding waves and the AO coupling coefficient, respectively. The phase mismatch, $\Delta\beta$ is expressed with L_B and Λ as follows:

$$\Delta\beta = 2\pi\left(\frac{1}{L_B(\lambda)} - \frac{1}{\Lambda}\right). \tag{3}$$

The coupled-mode equations in Eq. (2) can be analytically solved at resonance, i.e. when $\Delta\beta = 0$. For the vertically polarized input light, the initial conditions for electric fields are given by $E_1(0) = 1$ and $E_2(0) = 0$, and the coupled mode equation in Eq. (2) are solved as follows:

#220268 - $15.00 USD Received 1 Aug 2014; revised 18 Sep 2014; accepted 19 Sep 2014; published 24 Sep 2014

$$E_1(z) = \frac{1}{A} e^{-z(\alpha_1+\alpha_2)/4} \left[A\cos\left(\frac{Az}{4}\right) - (\alpha_1 - \alpha_2)\sin\left(\frac{Az}{4}\right) \right],$$
$$E_2(z) = \frac{4\kappa}{iA} e^{-z(\alpha_1+\alpha_2)/4} \sin\left(\frac{Az}{4}\right), \text{ where } A \equiv \sqrt{16\kappa^2 - (\alpha_1 - \alpha_2)^2}. \quad (4)$$

Here each modal power is defined by $P_i(z) \equiv |E_i(z)|^2$, and the calculated powers at resonance are plotted in Fig. 2 as a function of the propagation length, L. The blue solid and cyan dashed lines denote the modal powers of vertically polarized input mode and horizontally polarized coupled mode, respectively. The magenta dash-dotted line also represents total power of them. As shown in Fig. 2(a), when both modes are propagation modes (i.e. $\alpha_1 = \alpha_2 = 0$), each modal power competes with each other with π-phase difference since both modes continue coupling and exchanging their powers in every L while propagating along the fiber. In this case, total power stays constant along the fiber as long as there is no propagation loss. So in order to achieve band-rejection filtering, the coupled mode should be removed properly (e.g. through an output polarizer) as was in the cases of previous demonstrations. If the coupled mode become lossy however, i.e. $\alpha_2 > \alpha_1$, both of competing powers decay while propagating along the fiber as shown in Fig. 2(b) since overall modal powers participating in AO coupling fade along L due to the nonzero α_2. Only small fraction of the coupled power can be coupled back to the initial mode after experiencing high propagation loss, so that total power at resonance also decreases along L as shown in Fig. 2(b), leading to notch filtering performance of the proposed device without the requirement of extra polarizer. The linear loss coefficients used for calculations are $\alpha_1 = 0$ and $\alpha_2 = 30$ dB/m, which are realistic values in the state-of-the-art fiber manufacturing technology. The AO coupling coefficient used for calculations in Fig. 2 is $\kappa = 9.82\ \text{m}^{-1}$, which is a typical value feasible in our experimental setup described in the following section. The first four positions of the fiber when the input power is extinguished completely ($P_1 = 0$) are calculated to 0.181, 0.506, 0.831, 1.156 m, respectively [see Fig. 2(b)]. It means that the oscillation period of decaying power becomes longer at longer L, because the interacting powers of each mode contributing to AO coupling are unbalanced and weakened due to α_2 and thus require longer interaction lengths for complete power transfer. Note that in torsional AOTFs using typical low loss HB fibers, the oscillation periods are always constant as shown in Fig. 2(a). Total power extinction ratios calculated at resonance (i.e. expectable notch depths of the proposed scheme) corresponds to the magenta dash-dotted line in Fig. 2(b), which reach −20dB (0.01%) for L = 1.39 m and −30dB (0.001%) for L = 2.05 m, respectively. These long fiber lengths can be coiled to reduce overall device sizes as was in the case in [7] for practical applications.

In order to analyze transmission properties of the proposed AOTFs, we solve the coupled-mode equations in Eq. (2) numerically. The parameters used for calculations are: the resonant wavelength of λ_r = 1550 nm, the loss coefficients of $\alpha_1 = 0$ and $\alpha_2 = 30$ dB/m as is in the case of Fig. 2(b). For the phase mismatch term in Eq. (3), we considered the same dispersion of $L_B(\lambda)$ for the fiber used in the experiments described in the following section. Figure 3 shows the calculated transmission spectra of the proposed AOTF for several values of L. The first three values of L in Figs. 3(a)-3(c) (i.e. 0.506, 0.831, and 1.156 m) correspond to the second, third, and fourth points of the fiber length when the input power is extinguished completely ($P_1 = 0$) [see Fig. 2(b)]. We excluded the first point of L when $P_1 = 0$ because in this case total power extinction reaches −2.72dB at most and thus not so attractive. The blue solid, cyan dashed, and magenta dash-dotted lines in Fig. 3 represent the transmission curves of vertically polarized input mode, horizontally polarized coupled mode, and the sum of each mode, respectively. As indicated in Figs. 3(a)-3(c), the proposed AOTF already shows an excellent band-rejection performance with the power extinction of < −50dB at the given values of L. In order to exploit this property, however, the coupled mode should be removed properly by an output polarizer as was in the case of previous demonstrations. Without the polarizer, filter transmission curves are expressed as the sum of two polarization mode spectra, i.e. the

#220268 - $15.00 USD Received 1 Aug 2014; revised 18 Sep 2014; accepted 19 Sep 2014; published 24 Sep 2014

magenta dash-dotted lines in Fig. 3. Total power extinction at resonance improves at longer L and reaches −30dB when L = 2 m as indicated in Figs. 3(a)-3(d).

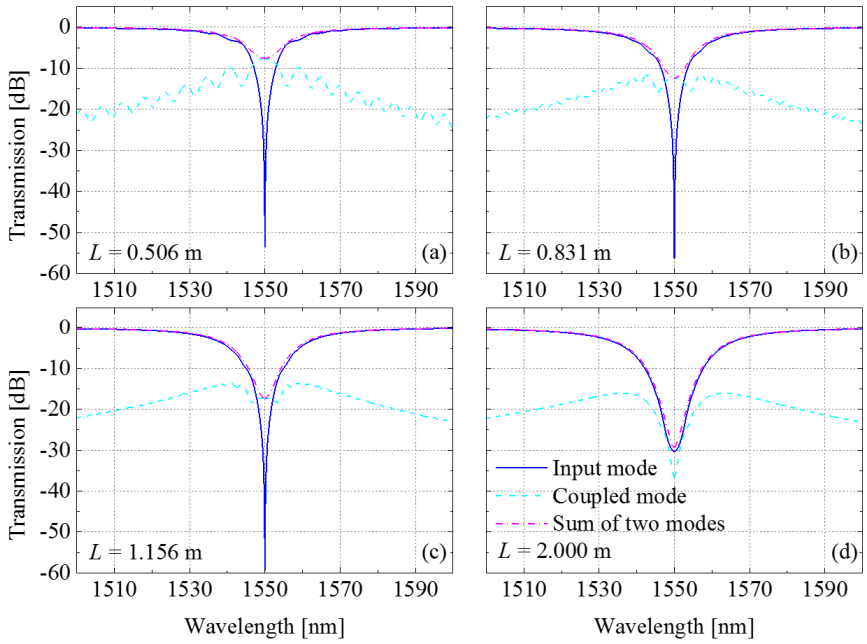

Fig. 3. Calculated filter transmission curves for several values of L. The blue solid, cyan dashed, and magenta dash-dotted lines represent the transmission curves of vertically polarized input mode, horizontally polarized coupled mode, and the sum of each, respectively.

Figure 4(a) plots the transmission spectra of the proposed scheme calculated for several different values of L chosen in Fig. 3 when an output polarizer is not used, showing excellent band-rejection filtering property. The calculated maximum extinction at resonance is plotted in Fig. 4(b) as a function of L. The fiber length should be longer than 2 m to obtain the power extinction less than −30dB, but we expect this long fiber length can be coiled to reduce the overall size as already mentioned above. As indicated in Fig. 4(b), the power extinction ratio at resonance (or the notch depth) is improved at longer fiber lengths, of which slope estimated by linear fitting is −15.03 dB/m. The simulation results also show that further power extinction is also feasible to −44.2dB at L = 3 m. Note that in torsional AOTFs using typical low loss HB fibers, the normalized total power of each mode at resonance as well as transmission curve always stay constant (at 0dB) without a polarizer to reject the coupled mode, as indicated in Fig. 2(a). The calculated 3dB-bandwidths of the proposed scheme become broader at longer L as can be seen in Fig. 4(a), since the lossy polarization mode components in both wings of the resonance dip satisfying the phase matching condition [Eq. (1)] suffer higher propagation loss at longer L. The calculated bandwidths are 33.3 nm for L = 2 m and 41.4 nm for L = 3 m, respectively [see the circular dotted blue line in Fig. 5(b)]. The 3dB-bandwidth is determined by the dispersion of L_B (λ) for the fiber as well as α_2, and thus can be tailored by adjusting these two design parameters to obtain particular spectral shapes. In contrast to the proposed scheme, the resonance dips become narrower at longer L in the previous torsional AOTFs using typical HB fibers, since the bandwidth is inversely proportional to L under the absence of propagation losses [15]. For comparison, we simulated the transmission curves for this case considering the same fiber parameters except the linear loss coefficients of $\alpha_1 = \alpha_2 = 0$. Figure 5(a) plots the corresponding results calculated for the same values of L chosen in Fig. 4(a), exhibiting the narrowing of resonance dips for longer L. Here in order to avoid over coupling between two interacting modes, we adjusted the AO coupling coefficient properly so that each L value can match with the exact fiber lengths for

#220268 - $15.00 USD Received 1 Aug 2014; revised 18 Sep 2014; accepted 19 Sep 2014; published 24 Sep 2014

complete power transfer from input eigen-polarization mode to the other eigen-mode. Note that an output polarizer is essential to obtain the transmission curves in Fig. 5(a) in contrast to the proposed scheme. The calculated 3dB-bandwidths of two schemes employing a single polarization fiber [Fig. 4(a)] and a HB fiber [Fig. 5(a)] are plotted together in Fig. 5(b) as a function of L, showing the opposite behavior to each other with increasing L. In the proposed scheme using a single polarization fiber, the bandwidth is not simply proportional to the inverse of L since the linear propagation loss of α_2 broadens the resonance dips further at longer L as described above and thus compensates the intrinsic bandwidth narrowing effect.

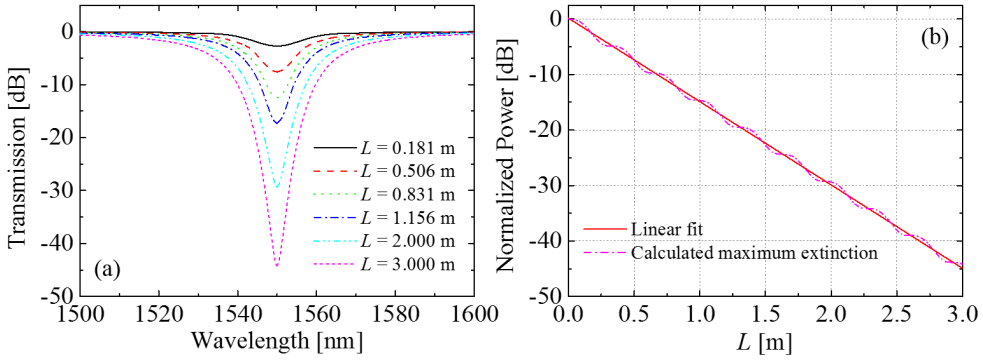

Fig. 4. (a) Calculated transmission spectra of the proposed scheme for several values of L when output polarizers are not used, and (b) calculated maximum extinction at resonance (or notch depth) plotted as a function of L. Its slope estimated by linear fitting is −15.03dB/m.

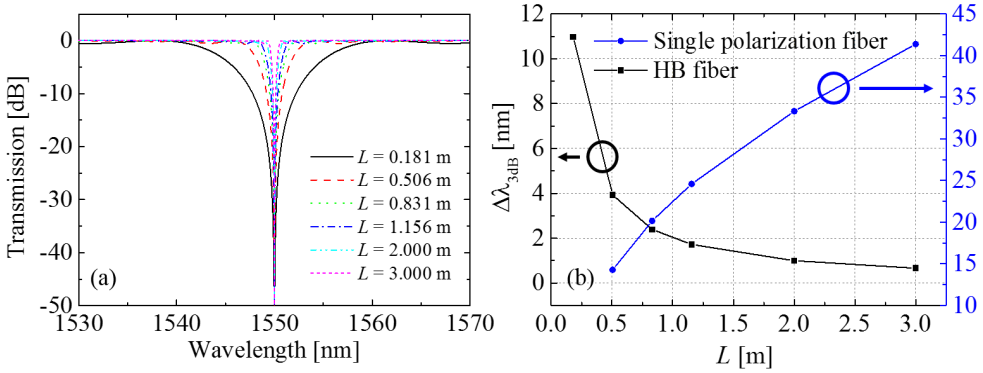

Fig. 5. (a) Calculated transmission spectra of the torsional AOTF using a HB fiber with the same fiber parameters for the case of Fig. 4(a) except the linear loss coefficients of $\alpha_1 = \alpha_2 = 0$. (b) Calculated 3dB-bandwidths of the torsional AOTFs using a single polarization fiber [Fig. 4(a)] and a HB fiber [Fig. 5(a)] plotted as a function of L.

In order to investigate the evolution of resonance dips along L more clearly, we calculated the spectral bandwidth of transmitted propagation mode for several values of α_2 and plotted the results in Fig. 6 as a function of L. Here the case of $\alpha_2 = 0$ corresponds to a typical HB fiber where both eigen-modes are all propagation modes, and the rest of cases with nonzero α_2 mean one of two eigen-mode is lossy and thus its power decays with increasing L. As shown in Fig. 6, the 3dB-bandwidths decrease with increasing L for two lowest values of α_2 because these cases are close to typical torsional AOTFs using HB fibers. For higher values of α_2 however, the widths rally after propagating a certain length of fiber because at which the influence of α_2 on bandwidth broadening becomes dominant and thus overcome the intrinsic bandwidth narrowing effect in a shorter fiber length. The results show that the 3-dB bandwidth can be tailored by adjusting the linear loss of the coupled mode (determined by the magnitude of α_2) in the proposed scheme. In general, the bandwidth can be tailored by

#220268 - $15.00 USD Received 1 Aug 2014; revised 18 Sep 2014; accepted 19 Sep 2014; published 24 Sep 2014

adjusting several design parameters including α_2, dispersion of polarization beat-length $L_B(\lambda)$ (or index dispersion of interacting modes, equivalently), and AO interaction length. As shown in Fig. 6, once the linear loss (α_2) and dispersion of $L_B(\lambda)$ are both determined, the optimum length of fiber to obtain the narrowest bandwidth can be sought. The dispersion of $L_B(\lambda)$ and α_2 are determined by the fiber geometry as well as the materials comprising fiber structure.

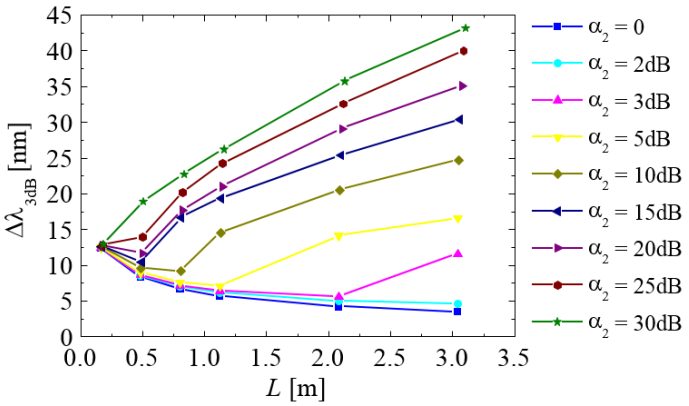

Fig. 6. Calculated 3dB bandwidths for the HB fiber with the different values of α_2.

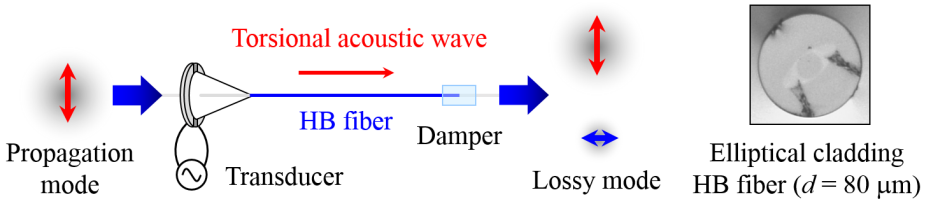

Fig. 7. Schematic diagram of the experimental setup that we used to validate our band-rejection filtering approach and associated model. Inset shows the cross-section view of the HB fiber used for measurements. The outer diameter of the bare fiber section is 80 μm.

3. Experimental results

Figure 7 illustrates a schematic diagram of the experimental setup that we used to validate our band-rejection filtering approach and associated model. The acoustic transducer to generate torsional acoustic wave comprises a combination of two pieces of shear mode lead zirconate titanate (PZT) plates vibrating with 180 degrees out of phase with each other. The PZT plates is attached to the bottom end facet of a cone-shaped glass horn with a hollow channel along its center axis, and a fiber penetrates through the channel from bottom to tip so that the generated torsional wave can be effectively coupled to the fiber at the tip. The cross-section of the HB fiber used in the experiment is also shown in the inset of Fig. 7. An elliptical stress member in the cladding region applies stress to the circular fiber core to produce high-birefringence, and the resulting polarization beat-length measured at λ = 1320 nm (continuous wave Nd:YAG laser) is 2.4 mm. The measured linear loss coefficients of two eigen-polarization modes are α_1 = 6.36 dB/m and α_2 = 23.46 dB/m, respectively. A small piece of sticky tape was attached at the end of AO interaction region of a bare section of the fiber, which operates as an acoustic damper to attenuate the applied torsional acoustic wave. Note that the proposed scheme in Fig. 7 is valid without the damper as we discussed in section 2. Here we used the damper to vary the AO interaction length (L) only when we measure the notch depth of transmission spectrum as a function of L. Input and output polarization modes are also depicted together in Fig. 7: propagation mode as red vertical arrows, lossy mode as a horizontal blue arrow, respectively. The input broadband light polarized parallel to the polarization axis of propagation mode is launched into the fiber, and then is coupled to the

#220268 - $15.00 USD Received 1 Aug 2014; revised 18 Sep 2014; accepted 19 Sep 2014; published 24 Sep 2014

other lossy eigen-polarization mode at the resonant wavelength via torsional AO coupling as described in Fig. 1. The coupled mode at resonance undergoes higher loss while propagating along the fiber, but the off-resonant propagation mode experiences the minimum loss as illustrated in Fig. 7.

In order to validate our theoretical model described in section 2, first we investigate the transmission properties of the propagation mode. Figure 8(a) shows the transmission curve of the off-resonant propagation mode measured at the applied RF frequency of 1.189 MHz (blue solid line). The bare fiber section used for AO interaction is 49.8 cm in length, which is close to the theoretical value of 49.3 cm that is the second point of L when the input power is extinguished completely ($P_1 = 0$) under our experimental conditions [see Fig. 8(b)]. For this measurement, we used an output polarizer to select the propagation mode only, and in this case the measured notch depth at resonance dip reaches −29.4dB. The 3-dB bandwidth of the measured spectrum is 8.6 nm, which is slightly narrower than the theoretical value of 9.36 nm where the dispersion of L_B (λ), the linear losses of each mode, and the AO coupling coefficient (κ) were considered properly [see the magenta dashed line in Fig. 8(a)]. The transducer driving voltage required for the maximum AO coupling efficiency in our setup is 10 V, which corresponds to $\kappa = 9.82$ m^{-1} in our model. The difference between calculated and measured bandwidths is thought to be due to non-uniformity in modal birefringence Δn in Eq. (1) [14]. Figure 8(b) plots the measured notch depth of the resonance dip as a function of L, which agrees well with the theoretical curve (blue solid line) plotted together in Fig. 8(b). The results show that the resonance dip oscillates and also deepens with increasing L as we discussed in Fig. 2(b), confirming the validity of our approach on band-rejection filtering and associated model. In light of the good agreement between our first proof-of-principle experiment and the theoretical predictions [Figs. 2, 3, and 8(b)], we can reasonably expect to reach a notch depth less than −30dB in longer fiber without both a damper and an output polarizer as expected in Fig. 4, from state-of-the-art torsional AO devices.

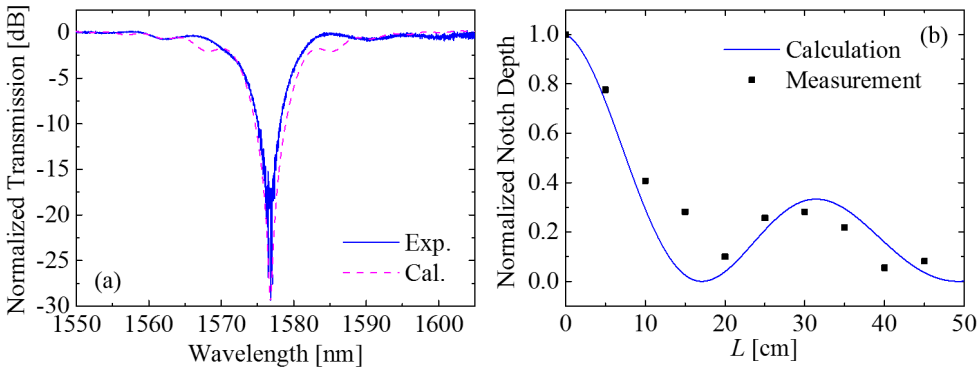

Fig. 8. (a) Transmission curves of the off-resonant propagation mode measured at the applied RF frequency of 1.189 MHz (blue solid line) and the calculated spectrum (magenta dashed line) where the same experimental parameters are considered, and (b) the measured and calculated notch depth of the resonant dip plotted as a function of L.

Finally we investigated the wavelength tunability of the proposed band-rejection filtering scheme. Here we removed the output polarizer, but kept the fiber jacket unstripped after the bare fiber AO interaction region to extinguish the coupled lossy mode effectively in a shorter length of fiber by absorption. Figure 9(a) shows the transmission spectra measured at several different RF frequencies, and the polarization dependence loss measured at the resonance dip is 0.8dB under our experimental conditions. The variation in resonant wavelength are plotted in Fig. 9(b) as a function of the applied RF frequency, exhibiting an almost linear relationship with the slope of 0.61 nm/kHz over the whole tuning range limited by the light source.

#220268 - $15.00 USD Received 1 Aug 2014; revised 18 Sep 2014; accepted 19 Sep 2014; published 24 Sep 2014

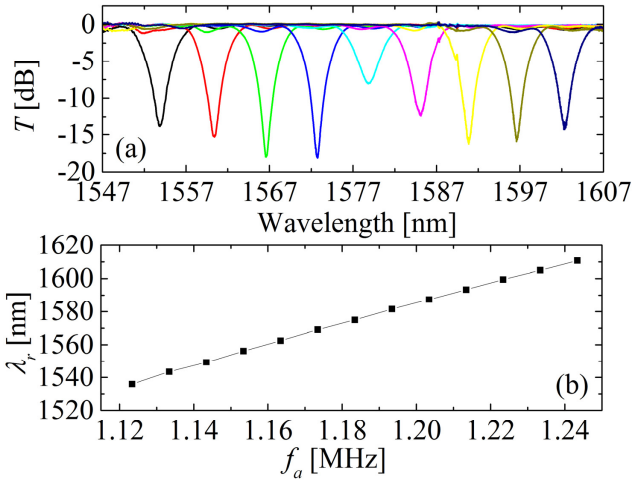

Fig. 9. (a) Transmission curves of the proposed AOTF measured at the various RF frequencies applied to the transducer, and (b) the measured resonant wavelength (λ_r) plotted as a function of the applied RF frequency (f_a), exhibiting a linear relationship.

4. Conclusion

We have theoretically investigated and experimentally demonstrated our novel band-rejection filtering scheme based on torsional AO coupling in a single polarization fiber. Our simulation results show that the polarization insensitive notch depth of −30dB is achievable for a 2-m-long fiber in the state-of-the-art fiber manufacturing technology. More efficient band-rejection in excess of −44dB could be also achieved in practical fiber length of 3 m which can be coiled to reduce the device size. The coiled fiber can be laid on an optical table (or any other non-sticky surface) allowing physical contact, thanks to torsional AOTFs' intriguing and unique property – immunity to external perturbation such as fiber bending or multiple contacts [7]. In this case, the axial strain along the fiber is zero, and thus any complicated packaging for the strain management is not required. If needed, either a piece of thin metal wire or a needle post can be one of good candidates as a non-sticky holder to sustain the AO interaction region. We verified the good agreement between our theoretical predictions and experimental band-rejection filtering performance, achieving a notch depth of −29.4dB for a low loss polarization mode after propagating the AO interaction length of 49.8 cm. The filtered wavelength could be tuned linearly by the variable RF transducer signal with the slope of 0.61 nm/kHz. The polarization dependence of notch depth measured without the polarizer was 0.8dB. Our proof-of-principle experiments show also the potential of the scheme as an all-fiber torsional AOTF with simpler device configuration not requiring extra polarizers and damper. Further significant improvements can be envisaged with fibers with the proper linear loss coefficients and dispersion of modal birefringence, enabling deeper notch depth in shorter fiber length. We highlight the proposed scheme will be a good foundation to develop the first mid-infrared in-fiber AO devices exploiting existing fiber-based device technologies in tele-communication band.

Acknowledgments

This research was supported by Basic Science Research Program through the National Research Foundation of Korea (NRF) funded by the Ministry of Science, ICT & Future Planning (NRF-2014R1A1A1002020), (2013R1A1A2064061) and the framework of international cooperation program managed by NRF of Korea (NRF-2013K2A1A2055029).

#220268 - $15.00 USD Received 1 Aug 2014; revised 18 Sep 2014; accepted 19 Sep 2014; published 24 Sep 2014